PERGAMON

Available online at www.sciencedirect.com

SCIENCE DIRECT®

International Journal of Multiphase Flow 29 (2003) 23–49

International Journal of Multiphase Flow

www.elsevier.com/locate/ijmulflow

Eulerian–Eulerian two-fluid model for turbulent gas–liquid bubbly flows

J. Chahed [a], V. Roig [b], L. Masbernat [b]

[a] *Ecole Nationale d'Ingénieurs de Tunis, BP No. 37, 1002 Le Belvédère, Tunis, Tunisia*
[b] *Institut de Mécanique des Fluides de Toulouse, Avenue Camille Soula, 31400 Toulouse, France*

Received 14 November 2000; received in revised form 17 September 2002

Abstract

The Eulerian–Eulerian two-fluid model presented in this paper emphasizes two aspects of the dynamic interactions between phases. First, the turbulent correlations associated with the added mass force are taken into account in the expression of the force exerted by the liquid on the bubbles, thus proving that the turbulent contributions of the interfacial transfer are significant in the phase distribution phenomena. Second, a turbulence model adapted to bubbly flows is developed. In this model, the Reynolds stress tensor of the continuous phase is split into two parts, a turbulent dissipative part produced by the gradient of mean velocity and by the wakes of the bubbles and a pseudo-turbulent non-dissipative part induced by the displacements of the bubbles: each part is predetermined by a transport equation. The application of the model to the simulation of three basic bubbly flows (grid, uniform shear and bubbly wake) confirms the pertinence of the improvements proposed for the closures of turbulence and of interfacial transfer. Comparison of the numerical results with the experimental data shows a good prediction of the mean and fluctuating velocities and of the phase distributions.
© 2002 Elsevier Science Ltd. All rights reserved.

Keywords: Two-phase flow; Bubbly flow; Two-fluid model; Turbulence model; Interfacial transfer; Phase distribution; Void fraction; Turbulent viscosity

1. Introduction

Many industrial processes in chemical, environmental and power engineering employ gas–liquid systems that are often designed to bring about transfer and transformation phenomena in two-phase flows. From a practical point of view, the development of general models which are able to predict the fields of average kinematic properties of both the gas and liquid phases and their presence rates in two-phase flows is of great interest for the design, control and improvement

0301-9322/03/$ - see front matter © 2002 Elsevier Science Ltd. All rights reserved.
PII: S0301-9322(02)00123-4

of gas–liquid systems. From a scientific point of view, the study of two-phase flows raises a number of challenging questions that still require theoretical advances and new experimental investigations.

New bubbly flow experiments, in a number of basic configurations, have been carried out over the last decades. The experimental investigations of gas–liquid bubbly flows show that the presence of the dispersed phase considerably alters the liquid turbulence. The bubbles induce turbulent fluctuations that enhance the global liquid turbulence level and alter the mechanisms of production, redistribution and dissipation of turbulence. In homogeneous and in some free bubbly flows (jet, mixing layer and wake), an enhancement of the liquid turbulence has been observed in comparison to equivalent single-phase flows (Lance and Bataille, 1991; Roig et al., 1998). In pure shear flow and in some wall bounded bubbly flows (boundary layer, pipe flows) a marked reduction of the turbulent shear stress has been observed, accompanied, at times, with an attenuation of the turbulent intensities (Lance et al., 1991; Moursali et al., 1995; Liu and Bankoff, 1990; Serizawa et al., 1992).

Knowledge of the presence rate of each phase in the two-phase flow field is of great importance, since it determines the amount of interfacial exchange. In non-homogeneous bubbly flows, the distribution of the void fraction is governed by the effects of the turbulence and of the forces exerted by the liquid on the bubbles. Drew and Lahey (1982), Wang et al. (1987) pointed out that the turbulence of the liquid phase plays an important role in phase distribution. Bel Fdhila and Simonin (1992) showed that the turbulent contributions of the momentum interfacial transfer are also important in relation to the phase distribution in bubbly flow in a sudden expansion. On the other hand, various experimental results for wall-bounded bubbly flows (Moursali et al., 1995; Liu and Bankoff, 1990) have described the effect of the bubble size and initial conditions on the distribution of the void fraction.

Analysis of the experimental results has greatly enhanced our understanding of two-phase flow mechanisms and has contributed to the development of two-phase flow models. The development of Eulerian–Eulerian, two-fluid models has been mostly guided by the single-phase statistical approach based on single-point modelling of the turbulence. Although based on some mathematical principles of theoretical physics, the single-point closure methodology is also a phenomenological approach, essentially founded on intuition, on dimensional and scale analyses and on the physical interpretation of experiments. In this research this approach was used as a methodology for generating approximate, but coherent physical closures laws.

In spite of the progress achieved in the development of Eulerian–Eulerian, two-fluid models for bubbly flows, (Simonin and Viollet, 1989; Lee et al., 1989; Lopez de Bertodano et al., 1990; Bel Fdhila and Simonin, 1992; Lopez de Bertodano et al., 1994), some important difficulties subsist. In particular, the prediction of the phase distributions remains, in our opinion, limited by the inadequate modelling of the turbulence and of the interfacial forces.

In the Eulerian–Eulerian two-fluid model we present in this paper, we attempt to improve the two-fluid models by emphasizing two aspects of the interaction between phases:

- First, we introduced the turbulent correlations related to the added mass force into the expression of the force exerted by the liquid on the bubbles. These correlations proved to be of great importance for computation of the void fraction in non-homogeneous bubbly flows. Under these conditions, the momentum balance indicates that the turbulence acts on the bubbles

via the well-known pressure term but also via the turbulent correlations obtained by averaging the added mass force (Chahed and Masbernat, 1998a).

- Second, the Reynolds stress tensor of the continuous phase was split into two parts: a turbulent dissipative part produced by the mean velocity gradient and by the bubbles wakes, and a pseudo-turbulent non-dissipative part induced by bubbles displacements; each part was predicted from a transport equation (Chahed and Masbernat, 1998b).

Furthermore, the development of this statistical model in the framework of the single-point closure of the turbulence, turned out to be very useful for analysing the complexity of bubbly flow, in the sense that the development, evaluation and testing of the closures, and comparisons with the experimental results, were very helpful for understanding the physical phenomena involved in the interfacial interactions.

This paper describes the most important steps of the modelling and then discusses the application of the model to three basic turbulent bubbly flows: homogeneous bubbly flows, at first uniform (Lance and Bataille, 1991), then with a constant shear (Lance et al., 1991) and finally to a bubbly wake behind a splitter plate (Roig, 1993).

2. Eulerian formulation of mass and momentum balance equations

2.1. Instantaneous balance equations

For incompressible bubbly flows without mass transfer, the instantaneous mass balance equations in the liquid and in the gas are respectively:

$$\frac{\partial(1-\chi_G)\rho}{\partial t}+\frac{\partial(1-\chi_G)\rho u_j}{\partial x_j}=0 \quad \text{and} \quad \frac{\partial \chi_G \rho_G}{\partial t}+\frac{\partial \chi_G \rho_G u_{Gj}}{\partial x_j}=0 \tag{1}$$

where u_{Gj}, ρ_G, and χ_G are respectively the velocity, the density and the characteristic function of the gas phase ($\chi_G = 1$ in the gas and 0 in the liquid). To simplify, the subscript G is used for the gas phase and the subscript L is omitted for the liquid phase throughout the paper. Thus u, ρ and $(1-\chi_G)$ are respectively the velocity, the density and the characteristic function of the liquid phase. At each point where the liquid phase is present, the instantaneous momentum balance is:

$$(1-\chi_G)\left(\rho\frac{\widetilde{\mathrm{D}}}{\widetilde{\mathrm{D}}t}u_i=\frac{\partial}{\partial x_j}\sigma_{ij}+\rho g_i\right) \tag{2}$$

where $\widetilde{D}/\widetilde{D}t=\partial/\partial t+u_j(\partial/\partial x_j)$, σ_{ij} is the stress tensor and g_i is the acceleration of gravity.

For the specific case of bubbly flows, we neglect the acceleration and the weight of the gas as compared to the force exerted by the liquid on the bubbles because of the contrast of the densities $\rho_G \ll \rho$; so, in each point where the gas phase is present, the instantaneous momentum equation in the gas indicates that the volume density of the total force f_{Pi} exerted by the liquid on the bubbles is zero:

$$\chi_G f_{Pi}=0 \tag{3}$$

The instantaneous momentum balance (3) represents an Eulerian description of the movement of the gas. It expresses the interfacial transfer as a local density of the force exerted by the liquid on the bubbles. The common way of deriving closure relations for the interfacial transfer is based on the formulation of the force exerted by the liquid phase on a single isolated bubble. This method comes up against two principal difficulties. The first difficulty is related to the general expression for the force exerted by the liquid on an isolated bubble. The second difficulty concerns the conversion of the Lagrangian information contained in the expression of the force into an Eulerian formulation for the local momentum transfer.

Within the framework of the Stokes approximation, Maxey and Riley (1983) and Gatignol (1983) expressed the force exerted by the liquid on a spherical particle as a summation of a "non-perturbed" flow contribution (in which the volume of the bubble is occupied by the liquid) and a "perturbed" flow contribution (in which the bubble is present). For a dispersed gas–liquid flow, with bubbles of about a millimetre and more, Stokes' law is not valid and there is no rigorous general expression for this force. Nevertheless, some theoretical and numerical works (Auton et al., 1988; Rivero et al., 1991; Magnaudet et al., 1995) now allow the extension of the results obtained for small spherical particles. In particular, Rivero et al. (1991) have confirmed the value of 0.5 for the added mass coefficient for a large Reynolds number range; they also found that the Basset force can be neglected for the bubbles.

Let $f_{Pi}^{(0)}$ and $f_{Pi}^{(1)}$ be the densities of the forces due to the "non-perturbed" and to the "perturbed" flows and ϑ_B and $\partial\vartheta_B$ the volume and the surface of the bubble; the volume density of the total force exerted by the liquid on the bubble is expressed in the form:

$$f_{Pi} = f_{Pi}^{(0)} + f_{Pi}^{(1)} = \frac{1}{\vartheta_B} \iint_{\partial\vartheta_B} \left(\sigma_{ij}^{(0)} + \sigma_{ij}^{(1)}\right) n_j \, \mathrm{d}S \tag{4}$$

where $\sigma_{ij}^{(0)}$ and $\sigma_{ij}^{(1)}$ are the stress tensors of the "non-perturbed" and "perturbed" flows respectively. The notion of non-perturbed flow introduced here places the model of the force in the category of dilute bubbly flows in which hydrodynamic interactions among bubbles are neglected.

The density of the force due to the "perturbed" flow action $f_{Pi}^{(1)}$ is modelled by referring to the numerical simulation results cited above, notably those of Rivero et al. (1991). We adopted the following expression for the volume density of the force exerted on a spherical bubble in a dilute bubbly flow:

$$f_{Pi}^{(1)} = -\frac{3}{4}\rho \frac{C_D}{d} \left|\vec{u}_G - \vec{u}^{(0)}\right| (u_{Gi} - u_i^{(0)}) - \rho C_A \left(\frac{\tilde{\mathrm{d}}}{\tilde{\mathrm{d}}} u_{Gi} - \frac{\widetilde{\mathrm{D}}}{\widetilde{\mathrm{D}}} u_i^{(0)}\right) - 2\rho C_L (u_{Gj} - u_j^{(0)}) \omega_{ij}^{(0)} \tag{5}$$

where $\tilde{\mathrm{d}}/\tilde{\mathrm{d}}t = \partial/\partial t + u_{Gj}(\partial/\partial x_j)$, $u_i^{(0)}$ is the instantaneous velocity of the "non-perturbed" flow, and $\omega_{ij}^{(0)} = 1/2(\partial u_i^{(0)}/\partial x_j - \partial u_j^{(0)}/\partial x_i)$ its instantaneous vorticity tensor. In Eq. (5), appear, respectively, the instantaneous densities of the drag force (with the drag coefficient C_D), the added mass force (with the coefficient C_A) and the lift force (with the coefficient C_L).

2.2. Average balance equations

For each variable of the flow field Φ, we define the mean value $\overline{\overline{\Phi_G}}$ in the gas phase and the mean value in the liquid phase $\overline{\overline{\Phi}}$ as follows:

$$\alpha\overline{\overline{\Phi_G}} = \langle \chi_G \Phi_G \rangle \quad (1-\alpha)\overline{\overline{\Phi}} = \langle (1-\chi_G)\Phi \rangle \quad \alpha = \langle \chi_G \rangle \tag{6}$$

where $\langle\,\rangle$ is a statistical averaging operator that verifies the Reynolds rules and α is the local average void fraction. In the following, we use Φ'_G and Φ' to designate the fluctuating values of Φ in the gas and in the liquid respectively, defined by

$$(1-\chi_G)\Phi = (1-\alpha)\overline{\overline{\Phi}} + (1-\chi_G)\Phi' \quad \text{and} \quad \chi_G \Phi_G = \alpha\overline{\overline{\Phi_G}} + \chi_G \Phi'_G \tag{7}$$

The averaging of Eqs. (1)–(3), leads to the following equations:

$$\frac{\partial(1-\alpha)\rho}{\partial t} + \frac{\partial}{\partial x_j}((1-\alpha)\rho\overline{\overline{u_j}}) = 0 \quad \text{and} \quad \frac{\partial(\alpha\rho_G)}{\partial t} + \frac{\partial}{\partial x_j}(\alpha\rho_G\overline{\overline{u_{Gj}}}) = 0 \tag{8}$$

$$\rho(1-\alpha)\frac{D}{Dt}\overline{\overline{u_i}} = (1-\alpha)\frac{\partial\overline{\overline{\sigma_{ij}}}}{\partial x_j} - \frac{\partial}{\partial x_j}\left(\rho(1-\alpha)\overline{\overline{u'_i u'_j}}\right) + \rho(1-\alpha)g_i + \left\langle (1-\chi_G)\frac{\partial\sigma'_{ij}}{\partial x_j}\right\rangle \tag{9}$$

$$\langle \chi_G f_{pi}\rangle = \left\langle \chi_G \frac{1}{\vartheta_B}\iint_{\partial\vartheta_B}(\sigma^{(0)}_{ij} + \sigma^{(1)}_{ij})n_j\,dS\right\rangle = 0 \tag{10}$$

with the average material derivative $D/Dt = \partial/\partial t + \overline{\overline{u_j}}(\partial/\partial x_j)$.

The average volume density of the force exerted by the liquid on the bubble can also be written in the form of a volume integral:

$$\langle \chi_G f_{pi}\rangle = \left\langle \chi_G \frac{1}{\vartheta_B}\iiint_{\vartheta_B}\left(\frac{\partial\sigma^{(0)}_{ij}}{\partial x_j} + \frac{\partial\sigma^{(1)}_{ij}}{\partial x_j}\right)d\vartheta\right\rangle = \left\langle \chi_G\left(\overline{\frac{\partial\sigma^{(0)}_{ij}}{\partial x_j}}^{(\vartheta_B)} + \overline{\frac{\partial\sigma^{(1)}_{ij}}{\partial x_j}}^{(\vartheta_B)}\right)\right\rangle \tag{11}$$

In Eq. (11), $^{-(\vartheta_B)}$ is a volume-averaging operator applied to the volume of the bubble. We represent the stress tensors of the "perturbed" and "non-perturbed" flows as the sum of mean and fluctuating values, we commute statistical and volume averaging over each bubble, and we rewrite the local density of the force in the form:

$$\langle \chi_G f_{pi}\rangle = \alpha\overline{\frac{\partial}{\partial x_j}\overline{\overline{\sigma^{(0)}_{ij}}}}^{(\vartheta_B)} + \overline{\left\langle \chi_G\frac{\partial}{\partial x_j}\sigma'^{(0)}_{ij}\right\rangle}^{(\vartheta_B)} + \alpha\overline{\frac{\partial}{\partial x_j}\overline{\overline{\sigma^{(1)}_{ij}}}}^{(\vartheta_B)} + \overline{\left\langle \chi_G\frac{\partial}{\partial x_j}\sigma'^{(1)}_{ij}\right\rangle}^{(\vartheta_B)} = 0 \tag{12}$$

In the absence of interfaces in the "non-perturbed" flow, we can derive from Eq. (12):

$$\overline{\left\langle \chi_G\frac{\partial}{\partial x_j}\sigma'^{(1)}_{ij}\right\rangle}^{(\vartheta_B)} = \overline{\left\langle \chi_G\frac{\partial}{\partial x_j}\sigma'_{ij}\right\rangle}^{(\vartheta_B)} = -\alpha\overline{\frac{\partial}{\partial x_j}\overline{\overline{\sigma_{ij}}}}^{(\vartheta_B)} \tag{13}$$

For relatively small bubbles, we have assumed spatial homogeneity of the stress tensor at the scale of the bubble diameter d; thus Eqs. (12) and (13) express the average momentum balances for the gas and the liquid in the form:

$$\alpha\frac{\partial}{\partial x_j}\overline{\overline{\sigma^{(0)}_{ij}}} + \langle \chi_G f^{(1)}_{Pi}\rangle = 0 \tag{14}$$

$$\rho(1-\alpha)\frac{D}{Dt}\overline{\overline{u_i}} = \frac{\partial\overline{\overline{\sigma_{ij}}}}{\partial x_j} - \rho\frac{\partial}{\partial x_j}\left((1-\alpha)\overline{\overline{u'_i u'_j}}\right) + \rho(1-\alpha)g_i \tag{15}$$

In principle, Eqs. (14) and (15) are not fundamentally different from the classical two-fluid model formulation. However, the decomposition of the flow fields into "perturbed" and "non-perturbed" components produces simple forms of the momentum balance equations in the gas and in the liquid; these equations are easy to interpret in physical terms.

With respect to interfacial momentum transfer modelling, the common method consists in considering the mean contributions when the turbulent contributions are either completely ignored (Lee et al., 1989) or possibly represented by a global dispersion effect which is proportional to the void fraction gradient (Lance and Lopez de Bertodano, 1992; Morel, 1997). We will show that these representations are inadequate for predicting void faction in bubbly flows and we suggest introducing the turbulent contribution generated by the added mass force into the interfacial transfer term: this was previously suggested by Bel Fdhila and Simonin (1992). We shall see below that the turbulent contribution of the added mass force plays an important role in the interfacial transfer model, and consequently in the bubble migration phenomenon.

In the present model, the turbulent contributions of the drag and lift forces are left out: we admit that the turbulent effect of the drag force can be taken into account through a suitable formulation of the drag coefficient and we expect that the turbulent contribution of the lift is negligible, considering the relatively weak correlation between the fluctuation of velocity and that of the vorticity in the liquid (Tennekes and Lumley, 1972). The momentum transfer term employed here is:

$$\langle \chi_G f_{pi}^{(1)} \rangle = -\frac{3}{4}\rho\alpha\frac{C_D}{d}|\vec{u}_R|\overline{\overline{u_{Ri}}} - C_A\rho\alpha\left(\frac{d_G\overline{\overline{u_{Gi}}}}{dt} - \frac{D\overline{\overline{u_i^{(0)}}}}{Dt}\right) - \rho\alpha C_L\overline{\overline{u_{Rj}}}\left(\frac{\partial\overline{\overline{u_j^{(0)}}}}{\partial x_i} - \frac{\partial\overline{\overline{u_i^{(0)}}}}{\partial x_j}\right) - C_A\rho\left\langle\frac{\partial}{\partial x_j}\chi_G\left(u'_{Gi}u'_{Gj} - u_i'^{(0)}u_j'^{(0)}\right)\right\rangle \tag{16}$$

where $\vec{u}_R$ is the relative velocity of the bubble defined by:

$$\alpha\overline{\overline{u_{Ri}}} = \langle\chi_G(u_{Gi} - u_i^{(0)})\rangle = \alpha(\overline{\overline{u_{Gi}}} - \overline{\overline{u_i}}) - \langle\chi_G u_i'^{(0)}\rangle \tag{17}$$

The last term in Eq. (17) represents a correlation between the velocity fluctuation in the "non-perturbed" flow and the instantaneous phase distribution. This term is modelled as a drifting velocity that takes into account the dispersion effect due to bubble transport by the turbulent fluid motion (Simonin and Viollet, 1989).

Eqs. (8), (14) and (15), together with the interfacial term (Eq. (16)) and the relative velocity (Eq. (17)), allow us to compute the average fields of void fraction α, velocities $\overline{\overline{u_i}}$ and $\overline{\overline{u_{Gi}}}$ and pressure $\overline{\overline{p}}$, provided that we build models for the viscous stress tensor and for the turbulent correlations $\overline{\overline{u_i'u_j'}}$, $\langle(\partial/\partial x_j)\chi_G(u'_{G,i}u'_{G,j} - u_i'^{(0)}u_j'^{(0)})\rangle$ and $\langle\chi_G u_i'^{(0)}\rangle$. In the following, we consider dilute gas–liquid bubbly flows and we relate the velocity and the stress tensor of the "non-perturbed" flow to that of the liquid phase.

The turbulent correlations produced by the added mass force contain turbulent correlations in the liquid and in the gas which means we had to develop a turbulence model for each of them. It should be observed that for homogeneous bubbly flows, the turbulent term resulting from the added mass force disappears; consequently the turbulence in the gas does not have to be modelled. For non-homogenous bubbly flows (e.g. bubbly wake behind a splitter plate), the turbulent

correlations for the gas were fitted to those of the liquid by means of the data obtained in the experiments: in these experiments the turbulent fluctuations of the bubbles were measured and were correlated to the liquid turbulence (Roig et al., 1998). Generally speaking, we assume that the dispersed phase turbulence can be related to the liquid turbulence through a turbulent dispersion model, based for example, on the Tchen theory in homogenous flow (Hinze, 1975) and on more recent works that take into account the non-homogeneity and crossing trajectory effects (Bel Fdhila and Simonin, 1992). Under these conditions, we had to develop a suitable model for the turbulence in the liquid.

3. Liquid turbulence modelling in bubbly flows

3.1. Transport equation for the Reynolds stress tensor

Several experiments have shown the important effect of interfacial interactions on the structure of turbulence in the liquid in bubbly flows (Wang et al., 1987; Lance et al., 1991; Moursali et al., 1995; Liu and Bankoff, 1990; Serizawa et al., 1992). These experimental results show that the interfaces, by modifying the characteristic scales of the turbulence, alter the different mechanisms (e.g. production, redistribution and dissipation). Therefore, the closure of the second-moment equations is, in our opinion, a minimal level for turbulence modelling if one is striving for a correct representation of these interfacial effects. Models of lower levels will appear as a reduction, under some conditions, of more general validated closures.

The Reynolds stress tensor transport equations can be obtained rigorously in two-phase flow (Lance, 1986):

$$
\begin{aligned}
\underset{(1)}{(1-\alpha)\frac{\mathrm{D}}{\mathrm{D}t}\overline{\overline{u_i'u_j'}}} = &\underset{(2)}{-(1-\alpha)\left(\overline{\overline{u_j'u_k'}}\frac{\partial\overline{\overline{u_i}}}{\partial x_k}+\overline{\overline{u_i'u_k'}}\frac{\partial\overline{\overline{u_j}}}{\partial x_k}\right)} \underset{(3)}{-2\nu(1-\alpha)\overline{\overline{\frac{\partial u_i'}{\partial x_k}\frac{\partial u_j'}{\partial x_k}}}} + \nu\overline{\overline{\frac{\partial}{\partial x_k}(u_i'u_j'n_k\delta^I)}} \\
&\underset{(4)}{-\frac{\partial}{\partial x_k}\left[(1-\alpha)\overline{\overline{u_i'u_j'u_k'}}-\nu\frac{\partial}{\partial x_k}\left((1-\alpha)\overline{\overline{u_i'u_j'}}\right)+\frac{(1-\alpha)}{\rho}\overline{\overline{p'(\delta_{jk}u_i'+\delta_{ik}u_j')}}\right]} \\
&\underset{(5)}{+\frac{(1-\alpha)}{\rho}\overline{\overline{p'\left(\frac{\partial u_i'}{\partial x_j}+\frac{\partial u_j'}{\partial x_i}\right)}}} \underset{(6)}{-\overline{\left(\frac{p'}{\rho}u_i'n_j+\frac{p'}{\rho}u_j'n_i\right)\delta^I+\nu\left(\frac{\partial}{\partial x_k}u_i'u_j'\right)n_k\delta^I}}
\end{aligned}
\tag{18}
$$

Except for the last term (term 6) which expresses the interfacial transfer (δ^I is a Dirac distribution over the interfaces), the other terms in the transport Eq. (18) have roughly the same meaning as in single-phase flow. The left-hand side term (term 1) represents the mean flow convection; on the right-hand side, we have, respectively, the mean shear production (term 2), the dissipation rate (term 3), the diffusion term (term 4), and the redistribution by the pressure fluctuations (term 5). The interfacial term can be seen as the power developed by the interfacial forces in the relative motion of the bubbles.

The turbulent stress tensor includes the shear induced fluctuations, the bubble induced fluctuations and their possible interactions. The bubble induced turbulence contains the non-dissipative

fluctuations resulting from the perturbation of the flow in the vicinity of the bubbles, and the fluctuations in the bubble wakes. The decomposition of these different mechanisms appears to be a realistic way of formulating theoretically acceptable closure laws with sufficient generality, in order to represent the different aspects of liquid turbulence in bubbly flows.

In their homogenous bubbly flow experiment, Lance and Bataille (1991) showed that the eddies produced in bubble wakes are dissipated by viscosity before their spectral transfer can take place. They demonstrated this by comparing the characteristic time scales for production, for dissipation in the bubble wakes and for spectral transfer of the turbulent energy. As pointed out by Lance and Bataille (1991), this hypothesis should be valid in the absence of strong acceleration of the bubbles due to large eddy transport. We assume that this result can be extended to cover a large range of bubbly flows.

This hypothesis is fundamental in turbulence modelling. Indeed, the interfacial production of turbulent energy by drag (a part of term (6) in Eq. (18)) and the dissipation rate in the bubble wakes (a part of term (3) in Eq. (18)) are balanced. Under these conditions, we may consider that the interfacial production of turbulent energy is reduced to the non-dissipative fluctuations induced by the perturbation of the flow in the vicinity of the bubbles.

We then decomposed the Reynolds stress tensor of the liquid into two independent parts: a turbulent part produced by the mean velocity gradient that also contains the turbulence of the bubble wakes (which is at equilibrium of production and dissipation) and a pseudo-turbulent part induced by bubble displacements. We thus write

$$\overline{\overline{u_i' u_j'}} = \overline{\overline{u_i' u_j'^{(\mathrm{T})}}} + \overline{\overline{u_i' u_j'^{(\mathrm{S})}}} \tag{19}$$

where (T) and (S) denote, respectively, the turbulent and pseudo-turbulent components. Such decomposition has been suggested by many experimental investigations (Lance and Bataille, 1991; Roig, 1993) and has been implemented into two-phase flow models (Lance et al., 1991; Lopez de Bertodano et al., 1994). The special feature of this turbulence modelling is the building of a specific transport equation for each part. The main purpose of this, is to specify each contribution in order to enable computation of the specific scales involved in the turbulence modelling of each part.

3.2. Transport equation for the turbulent part of the Reynolds stress tensor

The turbulent part of the Reynolds stress tensor $\overline{\overline{u_i' u_j'^{(\mathrm{T})}}}$ is produced by the mean shear and contains the turbulent fluctuations in the bubble wakes in particular those produced by the drag force in the relative movement. Under the hypothesis of the production-dissipation equilibrium in the bubble wakes, we do not have to specify explicitly the contribution of the wakes in the turbulent energy balance. The remaining dissipation is thus identified with isotropic dissipation at the small scales ε_0 which results from the energy cascade and the transport equation of the turbulent part of the Reynolds stress tensor $\overline{\overline{u_i' u_j'^{(\mathrm{T})}}}$ has the same form as in single-phase flow. Under these conditions, it is conceivable to expect that for a dilute dispersion of gas bubbles, the mechanisms that govern the turbulent part of the Reynolds stress tensor are similar to those in single-phase turbulence, provided that one develops adequate closures representing the interfacial effects on the

turbulence mechanisms. The transport equation for the turbulent part of the Reynolds stress tensor is symbolically written as follows:

$$\frac{\mathrm{D}}{\mathrm{D}t}\left(\overline{\overline{u_i' u_j'^{(\mathrm{T})}}}\right) = \mathrm{Diff}\left(\overline{\overline{u_i' u_j'^{(\mathrm{T})}}}\right) - \left(\overline{\overline{u_j' u_k'}}\frac{\partial \overline{\overline{u_i}}}{\partial x_k} + \overline{\overline{u_i' u_k'}}\frac{\partial \overline{\overline{u_j}}}{\partial x_k}\right) + \Phi_{ij}^{(\mathrm{T})} - \frac{2}{3}\varepsilon_0 \delta_{ij} \tag{20}$$

The convection and production terms do not need any closure laws, but we have to develop models for the diffusion $\left(\mathrm{Diff}(\overline{\overline{u_i' u_j'^{(\mathrm{T})}}})\right)$ and the redistribution ($\Phi_{ij}^{(\mathrm{T})}$) terms with specific closures for the effects due to the presence of the bubbles.

Just as for single-phase flow, the redistribution term is decomposed into a linear part and a non-linear part:

$$\Phi_{ij}^{\mathrm{T}} = (\Phi_{ij}^{(\mathrm{L})} + \Phi_{ji}^{(\mathrm{L})}) + (\Phi_{ij}^{(\mathrm{NL})} + \Phi_{ji}^{(\mathrm{NL})}) \tag{21}$$

The modelling of the redistribution term $\Phi_{ij}^{(\mathrm{T})}$ is based on the Lance et al. (1991) experimental data in pure shear bubbly flow. These authors noted a more pronounced tendency to isotropy in a two-phase flow; they explained this enhancement of isotropy by the supplementary stretching produced by the displacements of the bubbles. To take into account this effect, they modified the non-linear part of the single-phase redistribution model by modifying the time scale of turbulent stretching. We have adopted their suggestion and have rewritten the non-linear term in a slightly different form:

$$(\Phi_{ij}^{(\mathrm{NL})} + \Phi_{ji}^{(\mathrm{NL})}) = -C_1(\tau_{\mathrm{t}}^{-1} + \alpha\tau_{\mathrm{b}}^{-1})\left(\overline{\overline{u_i' u_j'^{(\mathrm{T})}}} - \frac{2}{3}k_0\delta_{ij}\right), \quad \text{where } k_0 = \frac{1}{2}\overline{\overline{u_i' u_i'^{(\mathrm{T})}}} \tag{22}$$

Contrary to the Lance et al. (1991) model, in which the entire turbulence in the liquid is considered, in this model we only consider, the turbulent part of the Reynolds stress tensor, thus avoiding inappropriate redistribution rates when the pseudo-turbulence is great. In Eq. (22), we introduced the time scale $\tau_{\mathrm{b}} = C_{\mathrm{R}}(d/|\vec{u}_{\mathrm{R}}|)$ related to the relative motion of the bubbles, and the characteristic time scale for turbulent eddy stretching $\tau_{\mathrm{t}} = k_0/\varepsilon_0$.

The linear part of the redistribution term $(\Phi_{ij}^{(\mathrm{L})} + \Phi_{ji}^{(\mathrm{L})})$ was modelled as for single-phase flow, and we adopted the model of Launder et al. (1975).

The diffusion terms in Eq. (20) and in the dissipation rate transport equation were modelled using a gradient law with a diffusion coefficient, which includes two effects: the turbulent diffusion tensor $\tau_{\mathrm{t}}\overline{\overline{u_k' u_l'^{(\mathrm{T})}}}$ expressed according to Launder et al. (1975) and the diffusion tensor associated with bubble motions. This one was modelled in the form $\tau_{\mathrm{b}}\overline{\overline{u_k' u_l'^{(\mathrm{S})}}}$, which "generalises" the Sato et al. (1981) model. With second-order turbulence modelling, the single-phase diffusion model of Launder et al. (1975) was thus "generalised" for two-phase bubbly flows in the form:

$$\mathrm{Diff}(\phi) = \frac{C_{\mathrm{s}\phi}}{(1-\alpha)}\frac{\partial}{\partial x_l}\left[(1-\alpha)\left(\tau_{\mathrm{t}}\overline{\overline{u_k' u_l'^{(\mathrm{T})}}} + \tau_{\mathrm{b}}\overline{\overline{u_k' u_l'^{(\mathrm{S})}}}\right)\frac{\partial \phi}{\partial x_k}\right] \tag{23}$$

3.3. Transport equation for the pseudo-turbulence

The transport equation for the non-dissipative, pseudo-turbulent stress tensor is symbolically written as:

$$\frac{\mathrm{D}}{\mathrm{D}t}\overline{\overline{u_i'u_j'^{(\mathrm{S})}}} = \mathrm{Diff}\left(\overline{\overline{u_i'u_j'^{(\mathrm{S})}}}\right) + \Phi_{ij}^{(\mathrm{S})} + P_{ij}^{(\mathrm{S})} \tag{24}$$

Without dissipation, the rhs of the transport equation for the pseudo-turbulent stress tensor contains, respectively, a diffusion, a redistribution and an interfacial production term.

For homogeneous, potential, bubbly flow, Biesheuvel and Van Wijngaarden (1984) have shown that bubble displacements create velocity fluctuations in the liquid phase, so the resulting pseudo-turbulent stress tensor is written as a function of the relative velocity and of the void fraction:

$$\overline{\overline{u_i'u_j'^{(\mathrm{S})}}} = \overline{\overline{u_i'u_{jH}'^{(\mathrm{S})}}} = \frac{3}{20}\alpha|\vec{u}_{\mathrm{R}}|^2\delta_{ij} + \frac{1}{20}\alpha\overline{\overline{u_{\mathrm{R}i}u_{\mathrm{R}j}}} \tag{25}$$

In inhomogeneous bubbly flows, we have no results for the generation of velocity fluctuations by bubble displacements so we used the following transport equation for the pseudo-turbulent contribution:

$$\frac{\mathrm{D}}{\mathrm{D}t}\overline{\overline{u_i'u_j'^{(\mathrm{S})}}} = \mathrm{Diff}\left(\overline{\overline{u_i'u_j'^{(\mathrm{S})}}}\right) + \frac{\mathrm{D}}{\mathrm{D}t}\overline{\overline{u_i'u_{jH}'^{(\mathrm{S})}}} \tag{26}$$

This equation states that the difference between pseudo-turbulence and the potential solution in homogeneous flow is a diffusive term associated with the non-homogeneous character of the flow. The last term in Eq. (26) can be interpreted as the contribution, in inhomogeneous flow, of the interfacial production by the added mass force $P_{ij}^{(\mathrm{S})}$ and of the redistribution by the pressure strain correlation $\Phi_{ij}^{(\mathrm{S})}$ with

$$P_{ij}^{(\mathrm{S})} = \frac{1}{2}\frac{\mathrm{D}}{\mathrm{D}t}\alpha\overline{\overline{u_{\mathrm{R}i}}}\,\overline{\overline{u_{\mathrm{R}j}}} \quad \text{and} \quad \Phi_{ij}^{(\mathrm{S})} = \frac{3}{10}(P_{kk}^{(\mathrm{S})})\delta_{ij} - \frac{9}{10}P_{ij}^{(\mathrm{S})} \tag{27}$$

For the diffusion terms in Eq. (26), we adopted the model in which we take into account the effects of the bubbles as indicated in Eq. (23).

The present model for pseudo-turbulence is not altogether general because Eq. (25) cannot give the amount of fluctuating kinetic energy induced in the general case of bubbly flow involving, for example, non-spherical and deformed bubbles. However, once the correct amount of pseudo-turbulence is produced by the model or given at the boundaries, from experimental data for example, Eq. (26) allows us to transport this variable and to compute the scales involved in two-phase turbulence.

4. Two-fluid model equations for almost-parallel flows

This section gives an overview of the two-fluid model equations in the case of almost parallel flows. As we simulated almost parallel two-dimensional flows, this treatment of the equations simplifies matters which is useful for further discussions.

4.1. Average balance of mass and momentum

For stationary, almost-parallel vertical bubbly flows we expressed the balance equation in the framework of the 2-D thin layer hypothesis (the ratio of diffusive and convective length scales is

small). We noted by $\overline{\overline{u}}$ and $\overline{\overline{v}}$, respectively, the vertical (direction x) and the transversal (direction y) components of the average velocities in the liquid and by (u', v') their corresponding fluctuations. In the following, we only retained the pressure in the stress tensor expression (we neglected the viscous stress tensor as compared to the turbulent one) and we made the velocity and pressure of the "non-perturbed" flow identical to those of the liquid phase.

Thus, for incompressible bubbly flows without mass transfer, the averaged mass balance equations in the liquid and in the gas are

$$\frac{\partial}{\partial x}(1-\alpha)\overline{\overline{u}} + \frac{\partial}{\partial y}(1-\alpha)\overline{\overline{v}} = 0 \quad \text{and} \quad \frac{\partial}{\partial x}\alpha\overline{\overline{u_G}} + \frac{\partial}{\partial y}\alpha\overline{\overline{v_G}} = 0 \tag{28}$$

The projection of the liquid momentum equation in the transverse direction reduces to

$$\frac{\partial}{\partial y}\left(\overline{\overline{p}} + \rho(1-\alpha)\overline{\overline{v'^2}}\right) = 0 \tag{29}$$

We introduced the modified pressure $P_e(x)$ as

$$P_e(x) = \overline{\overline{p}} + \rho g x + \rho(1-\alpha)\overline{\overline{v'^2}} \tag{30}$$

where g is the acceleration of gravity. Thus the longitudinal momentum balance in the liquid phase can be written as

$$(1-\alpha)\frac{D\overline{\overline{u}}}{Dt} = -\rho^{-1}\frac{dP_e(x)}{dx} - \frac{\partial}{\partial y}\left((1-\alpha)\overline{\overline{u'v'}}\right) + \alpha g \tag{31}$$

where

$$\frac{D}{Dt} = \overline{\overline{u}}\frac{\partial}{\partial x} + \overline{\overline{v}}\frac{\partial}{\partial y}$$

For bubbly flows with low void fractions, Eq. (31) indicates that the liquid movement is comparable to that of a single-phase flow in the presence of a buoyancy force $\rho\alpha g$. The two-phase flow specificity is of course related to the modification of the turbulent diffusion of the momentum by the presence of bubbles (second term on the rhs).

Within the boundary layer simplifications, the longitudinal and transversal projections of the momentum balance equations in the gas phase read respectively

$$0 = -\rho^{-1}\frac{dP_e(x)}{dx} - \frac{3}{4}\frac{C_D}{d}|\vec{u}_R|\overline{\overline{u_R}} - C_A\left[\left(\frac{d_G}{dt}\overline{\overline{u_G}} - \frac{D}{Dt}\overline{\overline{u}}\right) + \frac{1}{\alpha}\frac{\partial}{\partial y}\left(\overline{\overline{\alpha u'_G v'_G}} - \overline{\overline{\alpha u'v'}}\right)\right] + g \tag{32}$$

$$0 = \frac{\partial}{\partial y}(1-\alpha)\overline{\overline{v'^2}} - \frac{3}{4}\frac{C_D}{d}|\vec{u}_R|\overline{\overline{v_R}} - \frac{C_A}{\alpha}\frac{\partial}{\partial y}\left(\alpha\overline{\overline{v'^2_G}} - \alpha\overline{\overline{v'^2}}\right) - C_L\overline{\overline{u_R}}\frac{\partial\overline{\overline{u}}}{\partial y} \tag{33}$$

where

$$\frac{d_G}{dt} = \overline{\overline{u_G}}\frac{\partial}{\partial x} + \overline{\overline{v_G}}\frac{\partial}{\partial y}$$

and the longitudinal and the transversal relative velocities are:

$$\overline{\overline{u_R}} = (\overline{\overline{u_G}} - \overline{\overline{u}}) - \frac{1}{\alpha}\langle \chi_G u' \rangle \quad \text{and} \quad \overline{\overline{v_R}} = (\overline{\overline{v_G}} - \overline{\overline{v}}) - \frac{1}{\alpha}\langle \chi_G v' \rangle \tag{34}$$

In Eqs. (32) and (33), the Tchen force is expressed according to the Eq. (29) and the added mass force includes besides the average contributions (negligible in the transverse direction) the turbulent contributions that contain turbulent correlations in the liquid and in the gas. The lift force acts only in the transverse direction: with the almost-parallel flow hypothesis, the longitudinal projection of this term is negligible.

The correlation between the continuous phase velocity fluctuation and the instantaneous phase distribution in Eq. (34) is considered as a drift velocity which takes into account the dispersion effect due to bubble transport by turbulent fluid motion. Generally speaking, the ability of the bubble to respond to the surrounding fluctuations depends on its size, its density relative to the carrier fluid and on the turbulence structure of the continuous phase. The drift velocity is represented as a dispersion effect proportional to the void fraction gradient in which we introduce the crossing trajectories effect that describes the loss of correlation due to the mean relative velocity of the bubbles (Csanady, 1963). In almost-parallel flow, the longitudinal component of the drift velocity is negligible and we consider the following expression for the transversal one:

$$\langle \chi_G v' \rangle = -C_{DT} C_{sk} D_{yy} (1 + C_\beta \xi^2)^{-1/2} \frac{\partial \alpha}{\partial y} \tag{35}$$

where $D_{yy} = \tau_t \overline{\overline{v_t'^2}} + \tau_b \overline{\overline{v_s'^2}}$ (see Section 4.2) and $\xi = |\vec{u}_R|/\sqrt{k_0}$, C_β is a constant taken equal to 0.45 following Simonin and Viollet (1989).

It should be observed that the drift velocity has a similar effect as the void fraction dispersion term introduced, for example, by Lopez de Bertodano et al. (1990), in order to take into account the turbulent contribution in the interfacial transfer term. Hereafter we analyse this void fraction dispersion effect by varying the coefficient C_{DT} of the drift velocity.

Finally, the drag coefficient C_D is given by the expression of Wallis for spherical bubbles, (Clift et al., 1978):

$$\begin{aligned} C_D &= \frac{24}{R_e}(1 + 0.15 R_e^{0.687}), \quad R_e \leqslant 1000 \\ C_D &= 0.44, \quad R_e \geqslant 1000 \end{aligned} \tag{36}$$

R_e is the Reynolds number, based on the relative velocity and the bubble diameter.

4.2. Transport equations for the Reynolds stress tensor

The transport equations for the most important components of the Reynolds stress tensor in 2-D bubbly flows are modelled according to the second-order closure of the turbulence presented above and written in the framework of almost-parallel flow. The subscript (t) designates the turbulent part of the Reynolds stress tensor and the subscript (s) the pseudo-turbulent part. This gives:

$$\overline{\overline{u'^2}} = \overline{\overline{u_t'^2}} + \overline{\overline{u_s'^2}}, \quad \overline{\overline{v'^2}} = \overline{\overline{v_t'^2}} + \overline{\overline{v_s'^2}}, \quad \overline{\overline{u'v'}} = \overline{\overline{u_t'v_t'}} \quad \text{as} \quad \left(-\overline{\overline{u_s'v_s'}}\right) \Big/ \left(-\overline{\overline{u_t'v_t'}}\right) \ll 1 \tag{37}$$

The transport equations of the turbulent part of the Reynolds stress components are:

$$\frac{\mathrm{D}}{\mathrm{D}t}\overline{\overline{u_t'^2}} = \frac{C_{sk}}{(1-\alpha)}\frac{\partial}{\partial y}\left[(1-\alpha)D_{yy}\frac{\partial}{\partial y}\overline{\overline{u_t'^2}}\right] - C_1\left(\frac{\varepsilon_0}{k_0}+\alpha\tau_b^{-1}\right)\left(\overline{\overline{u_t'^2}}-\frac{2}{3}k_0\right) - 2\left(1-\frac{\gamma_1}{3}+\frac{2\gamma_3}{3}\right)\overline{\overline{u'v'}}\frac{\partial\overline{\overline{u}}}{\partial y}-\frac{2}{3}\varepsilon_0 \tag{38}$$

$$\frac{\mathrm{D}}{\mathrm{D}t}\overline{\overline{v_t'^2}} = \frac{C_{sk}}{(1-\alpha)}\frac{\partial}{\partial y}\left[(1-\alpha)D_{yy}\frac{\partial}{\partial y}\overline{\overline{v_t'^2}}\right] - C_1\left(\frac{\varepsilon_0}{k_0}+\alpha\tau_b^{-1}\right)\left(\overline{\overline{v_t'^2}}-\frac{2}{3}k_0\right) - \frac{2}{3}(2\gamma_1-\gamma_3)\overline{\overline{u'v'}}\frac{\partial\overline{\overline{u}}}{\partial y}-\frac{2}{3}\varepsilon_0 \tag{39}$$

$$\frac{\mathrm{D}}{\mathrm{D}t}\left(\overline{\overline{-u_t'v_t'}}\right) = \frac{C_{sk}}{(1-\alpha)}\frac{\partial}{\partial y}\left[(1-\alpha)D_{yy}\frac{\partial}{\partial y}\left(\overline{\overline{-u_t'v_t'}}\right)\right] - C_1\left(\frac{\varepsilon_0}{k_0}+\alpha\tau_b^{-1}\right)\left(\overline{\overline{-u_t'v_t'}}\right) + \left((1-\gamma_1)\overline{\overline{v'^2}}+\gamma_2 k-\gamma_3\overline{\overline{u'^2}}\right)\frac{\partial\overline{\overline{u}}}{\partial y} \tag{40}$$

where $\tau_b = C_R(d/|\vec{u}_R|)$ is the time scale related to the relative motion of the bubbles.

The transport equations of the components of the pseudo-turbulent part of the Reynolds stress tensor are also written in the framework of vertical almost-parallel flow approximation:

$$\frac{\mathrm{D}}{\mathrm{D}t}\overline{\overline{u_s'^2}} = \frac{C_{sk}}{(1-\alpha)}\frac{\partial}{\partial y}\left[(1-\alpha)D_{yy}\frac{\partial}{\partial y}\overline{\overline{u_s'^2}}\right] + \frac{4}{20}\frac{\mathrm{D}}{\mathrm{D}t}\alpha\overline{\overline{u_R}}^2 \tag{41}$$

$$\frac{\mathrm{D}}{\mathrm{D}t}\overline{\overline{v_s'^2}} = \frac{C_{sk}}{(1-\alpha)}\frac{\partial}{\partial y}\left[(1-\alpha)D_{yy}\frac{\partial}{\partial y}\overline{\overline{v_s'^2}}\right] + \frac{3}{20}\frac{\mathrm{D}}{\mathrm{D}t}\alpha\overline{\overline{u_R}}^2 \tag{42}$$

The dissipation rate at the small scale ε_0 resulting from the energy cascade is taken as isotropic according to the local isotropy hypothesis and computed from a similar single-phase transport equation:

$$\frac{\mathrm{D}\varepsilon_0}{\mathrm{D}t} = \frac{C_{s\varepsilon}}{(1-\alpha)}\frac{\partial}{\partial y}\left[(1-\alpha)D_{yy}\frac{\partial\varepsilon_0}{\partial y}\right] - C_{1\varepsilon}\frac{\varepsilon_0}{k_0}\overline{\overline{u'v'}}\frac{\partial\overline{\overline{u}}}{\partial y} - C_{2\varepsilon}\frac{\varepsilon_0^2}{k_0} \tag{43}$$

Except for the coefficient C_R that needs to be adjusted from the experimental data in order to bring up the supplementary stretching induced by the bubbles, the other constants of the bubbly flow turbulence model have the values currently adopted for second-order turbulence modelling of single-phase flows. It should be observed that the effect of the interfacial effects on the turbulence mechanisms has been modelled by developing supplementary closures, while the initial closure of the turbulence, with the constants adjusted for single-phase flow, has been conserved. The constants employed here are given in Table 1.

Table 1
Constants of the turbulence model

γ_1	γ_2	γ_3	C_{sk}	$C_{s\varepsilon}$	C_1	$C_{1\varepsilon}$	$C_{2\varepsilon}$
0.76	0.18	0.11	0.11	0.15	1.8	1.44	1.92

A two-dimensional numerical code has been developed for parabolic flow resolution. The numerical method is based on a finite-difference scheme and the equations are solved with an explicit method.

5. Results and discussion

5.1. Homogeneous bubbly flows

The study of homogeneous flows is interesting for the analysis of turbulence in bubbly flows because it allows us to avoid the difficulties related to the heterogeneity of void fraction distribution and diffusion effects. Therefore it is possible, in this particular case, to focus on the analysis of the effects of bubbles on turbulence production and redistribution mechanisms. Lance and Bataille (1991) and Lance et al. (1991) carried out experiments in two vertical, homogeneous air–water bubbly flows (grid flow and pure shear flow). These experiments were conducted in a hydrodynamic tunnel with a test section consisting of a 2 m long, square channel (450×450 mm). The uniform shear was created by adjusting the head loss in the inlet section.

For each bubbly flow, we had to define adequate inlet conditions. Thus we first simulated the corresponding single-phase flow. The inlet conditions of the turbulent energy and of its dissipation rate were adjusted at the inlet section in order to obtain a suitable prediction of the longitudinal evolution of the components of the Reynolds stress tensor as compared to the experimental data in this single-phase flow. Then, in the two-phase flow simulations, the relative velocity of the gas was set equal to zero throughout the inlet section: the pseudo-turbulence was consequently zero and the turbulence was taken to be that of the single-phase data.

5.1.1. Evolution of the turbulent intensities

Fig. 1 shows the computed and measured turbulent intensities in uniform single-phase flow ($U = 0.6$ m/s) and in three uniform bubbly flows ($\alpha = 0.005$, 0.01 and 0.02). These results show that the decay of the turbulence behind the grid is in good agreement with the experimental data and indicate that the Reynolds stress tensor in bubbly flow is well predicted by our model. The acceleration of the bubbles from zero slip velocity at the inlet to their terminal velocity takes place over a very short distance and produces the correct amount of pseudo-turbulence through the added mass effects. It should be observed that the bubble terminal relative velocity produced by the model is larger than the experimental value given by Lance and Bataille (1991). In the experiment, the bubbles had an oblate spheroidal shape with a mean equivalent diameter equal to 5 mm and a helicoidal trajectory. In the interfacial force model, we considered spherical bubbles with standard coefficients for the drag and added mass forces. This explains why the slip velocity is over predicted, but the amount of the pseudo-turbulence is well produced with a standard added mass coefficient lower than the experimental one. It should be possible to take into account the effects of the deformation and of the instability of the trajectory by a simultaneous modification of the drag and added mass forces, as suggested by Lance and Lopez de Bertodano (1992).

Figs. 2 and 3 also indicate good agreement between simulations and data in single-phase pure shear flow and in a bubbly flow ($\alpha = 0.01$), respectively, with the same mean velocity and the same shear intensity ($U = 1$ m/s, $S = 2.9$ s^{-1}, respectively). The new redistribution term modelling is

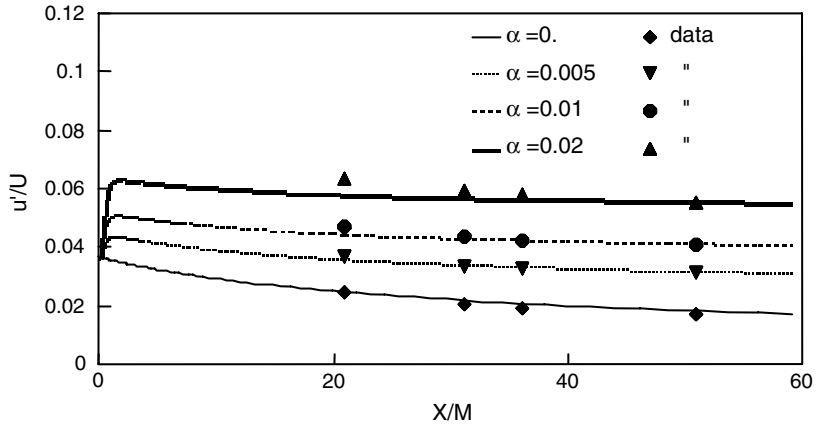

Fig. 1. Decay of the turbulent intensities in homogeneous uniform bubbly flow. Comparison of the numerical results with the experimental data of Lance and Bataille (1991). (X is the distance from the grid, U is the uniform velocity and M is the size of the mesh.)

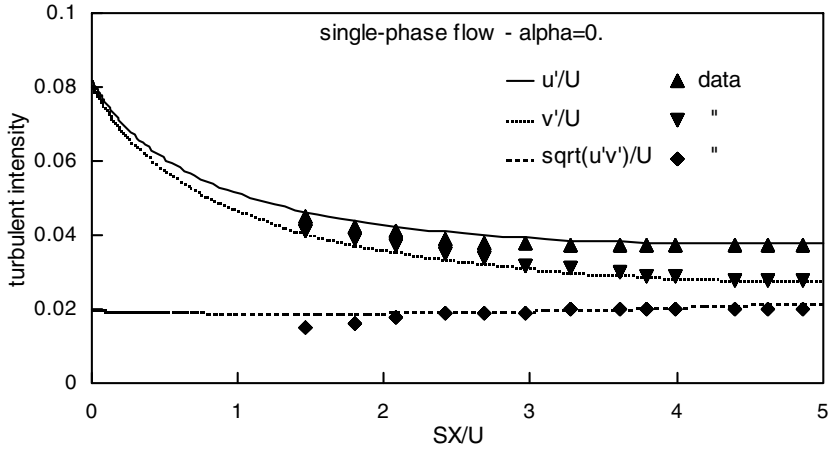

Fig. 2. Turbulence in pure shear single-phase flow. Comparison of the numerical results with the experimental data of Lance et al. (1991). (X is the distance from the inlet, U is the average velocity over the experimental section and S is the shear intensity $S = \mathrm{d}u/\mathrm{d}y$.)

tested in this flow configuration and the value of the coefficient C_R has been adjusted to 2/3. This value, which reproduces correctly the turbulent stress tensor and the supplementary amount of the isotropy observed in pure shear bubbly flow experiments with different void fractions ($\alpha = 0.005$, 0.01, 0.014 and 0.02), has been maintained in all the following simulations of inhomogeneous bubbly flows.

5.1.2. A new turbulent viscosity formulation for bubbly blows

The model reproduces a slight reduction of the shear stress and an enhancement of the total turbulent energy in the pure shear bubbly flow in comparison with single-phase flow. Since the

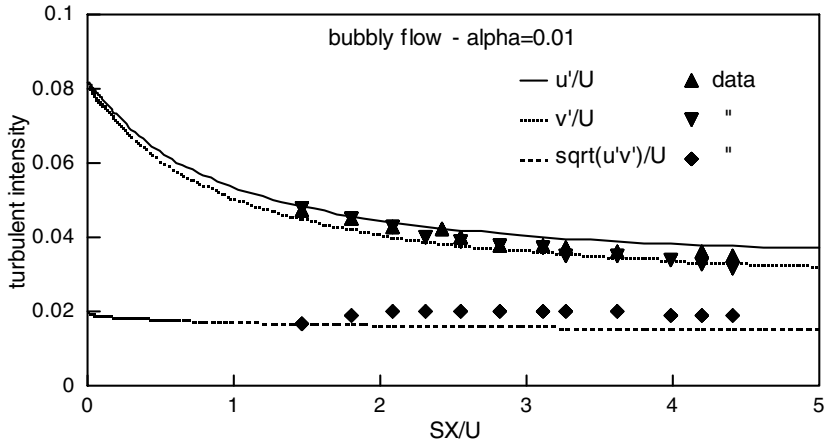

Fig. 3. Turbulence in pure shear bubbly flow. Comparison of the numerical results with the experimental data of Lance et al. (1991). (X is the distance from the inlet, U is the average velocity over the experimental section and S is the shear intensity $S = \mathrm{d}u/\mathrm{d}y$.)

shear intensity is the same in both single-phase and bubbly flows, the attenuation of the turbulent shear stress in bubbly flow can be interpreted as a reduction of the turbulent viscosity, and the present turbulence model correctly reproduces this result. Indeed, the simplified balance between production and redistribution in the shear stress transport equation (Eq. (40)), allows us to obtain an explicit expression of the turbulent shear stress that clearly shows the mechanisms by which the turbulent viscosity is altered by the presence of bubbles:

$$\overline{\overline{-u'v'}} \approx \overline{\overline{-u'_{\mathrm{t}}v'_{\mathrm{t}}}} = \frac{\left((1-\gamma_1)\overline{\overline{v'^2}} + \gamma_2 k - \gamma_3 \overline{\overline{u'^2}}\right)}{C_1\left(\frac{\varepsilon_0}{k_0} + \alpha\tau_{\mathrm{b}}^{-1}\right)} \frac{\partial \overline{\overline{u}}}{\partial y} \tag{44}$$

The turbulent terms in the numerator of Eq. (44) are split into turbulent and pseudo-turbulent contributions and we postulate:

$$\left((1-\gamma_1)\overline{\overline{v'v'}} + \gamma_2 k - \gamma_3 \overline{\overline{u'u'}}\right) = C_1(C_{\mu 0}k_0 + C_{\mu \mathrm{b}}k_{\mathrm{S}}) \tag{45}$$

where $k_{\mathrm{S}} = \frac{1}{2}\overline{\overline{u'_i u'^{(\mathrm{S})}_i}}$ is the pseudo-turbulent part of the energy. $C_{\mu 0}$ and $C_{\mu b}$ are coefficients depending on the turbulence and pseudo-turbulence anisotropy. Eqs. (44) and (45) yield the following expression for the turbulent viscosity:

$$v_{\mathrm{t}} = C_\mu \frac{k_0^2}{\varepsilon_0} \frac{\left(1 + \frac{C_{\mu b}}{C_{\mu 0}}\frac{k_{\mathrm{S}}}{k_0}\right)}{\left(1 + \alpha\frac{\tau_{\mathrm{t}}}{\tau_{\mathrm{b}}}\right)} = v_{t0} \frac{\left(1 + \frac{C_{\mu b}}{C_{\mu 0}}\frac{k_{\mathrm{S}}}{k_0}\right)}{\left(1 + \alpha\frac{\tau_{\mathrm{t}}}{\tau_{\mathrm{b}}}\right)} \tag{46}$$

This turbulent viscosity formulation, derived from a reduction of the transport equation of the Reynolds stress tensor, conserves the physical contents of second-order closure modelling. It accounts for the mechanisms by which the turbulent shear stress of the liquid phase is altered by the presence of the bubbles. Eq. (46) expresses two competing interfacial effects that govern the

turbulent viscosity in bubbly flows: agitation of the bubbles causes, on the one hand an enhancement of the turbulence and of the resulting shear stress (numerator of Eq. (46)); on the other hand it induces a modification of the characteristic scale of the eddy stretching that causes more isotropy of the turbulence with an attenuation of the shear stress (denominator of Eq. (46)). As a result, depending on which of these two effects dominates, the turbulent shear stress in bubbly flow can be more or less important than the corresponding one in the equivalent single-phase flow. When the turbulent shear stress is reduced, turbulence production by the mean velocity gradient is lower and we may obtain an attenuation of the turbulence as observed, under certain conditions, in some wall bounded bubbly flows (Wang et al., 1987; Liu and Bankoff, 1990; Serizawa et al., 1992). Indeed, the turbulent viscosity formulation provides an easy means of correctly representing the shear stress in bubbly flows with a two-equation turbulence model. We showed that such a two-equation turbulence model is able to represent the effects of the bubbles on the turbulence mechanisms and to correctly reproduce the varying behaviour of the turbulence structure in the liquid phase of bubbly flows. It is also able to explain the possible attenuation of the turbulence, (Chahed et al., 1999; Chahed and Masbernat, 2001).

The turbulent viscosity model proposed by Sato et al. (1981) cannot reproduce the possible attenuation of the turbulent shear stress as observed in some bubbly flows. Indeed, according to this model, the turbulent viscosity of the bubbly flow is always greater than the turbulent viscosity in the equivalent single-phase flow. This model reads:

$$\nu_t = \nu_{t0} + C_b \alpha d |\vec{u}_R| \tag{47}$$

Fig. 4 shows the turbulent viscosity resulting from our second-order turbulence model (Eq. (46)) compared to the model by Sato et al. (1981) (Eq. (47)). It appears that the turbulent viscosity generated by our turbulence modelling is smaller than the turbulent viscosity of the single-phase flow. On the other hand, with the Sato model, the turbulent viscosity in bubbly flow is constantly

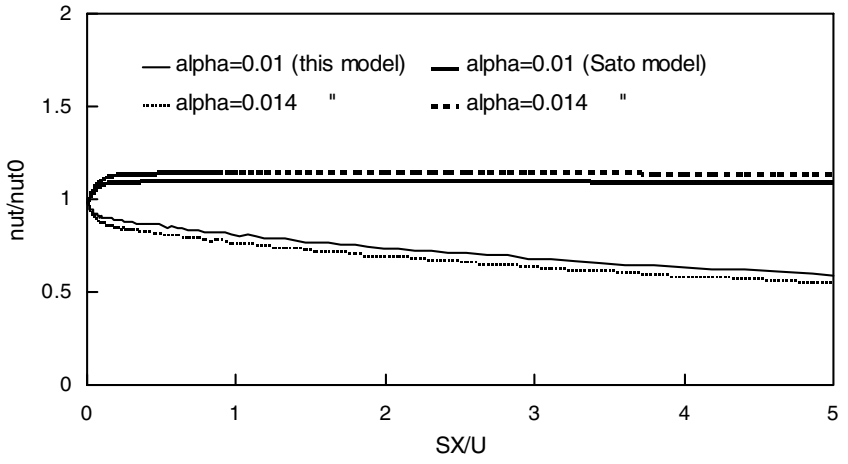

Fig. 4. Ratio of the "two-phase" flow turbulent viscosity to the "single-phase" one in pure shear flow. Comparison of the numerical results with Sato et al. model (1981). (X is the distance from the inlet, U is the average velocity over the experimental section and S is the shear intensity $S = \mathrm{d}u/\mathrm{d}y$.)

greater than that in the equivalent single-phase flow and the model cannot reproduce the attenuation of the turbulent shear stress, as observed in the experiment.

5.2. Vertical bubbly wake

The two-fluid model is also applied to a plane vertical bubbly wake and the numerical results are confronted with the experimental data of Roig (1993). In this experiment, the bubbly wake is produced by the confluence of two similar uniform bubbly flows separated by a splitter plate (thickness 2 mm). Measurements of mean and RMS velocities of the liquid phase in the longitudinal direction were performed using a hot film anemometer. The mean and RMS velocities in the gas phase and also the void fraction were measured using a double optical probe. The bubbly wake is roughly characterised by the following parameters: mean velocity of the liquid 0.6 m/s, mean void fraction 2% and mean equivalent bubble diameter 3 mm (the bubbles are not spherical).

As for homogenous flows, we first began by simulating the single-phase flow: in this simulation, the inlet conditions for the average velocity and the turbulence were fixed from the single-phase experimental data at $X = 0.01$ m before the edge of the splitter plate and the dissipation rate was adjusted so that we obtained a good prediction of the flow development as compared to the experimental data.

In the two-phase flow simulation, we also fixed the average liquid velocity and the liquid turbulence at the inlet section on the basis of the experimental data and likewise for the void fraction. In order to specify the turbulent and pseudo-turbulent contributions, we related the turbulent part to the single-phase turbulence measurements at the inlet section: this initialisation, which appears intuitive to some extent, was validated by the good behaviour of the turbulence model in this flow configuration. For the gas phase, the average gas velocity at the inlet section was computed as the summation of the mean liquid velocity and the computed terminal velocity of the bubbles, and the turbulent stress tensor was set proportional to the liquid one through a proportionality factor based on experimental data. It should be observed that the experimental profiles of the average and RMS velocities and of void fraction in the inlet section are not perfectly symmetrical probably because of the non-uniformity of the injection conditions. However, the inlet conditions, mostly based on the experimental data, implicitly took this lack of symmetry of the flow into account in the boundary condition at the inlet section.

5.2.1. Prediction of the average and fluctuating liquid velocities

Figs. 5 and 6 show good agreement between the numerical results for the mean liquid velocity and the experimental data in the single phase and in the bubbly wakes at $X = 0.2$ and 0.3 m from the splitter plate. In these figures, we observe a significant enhancement of the momentum spread in bubbly flow as compared to the equivalent single-phase flow. This result suggests that the turbulent shear stress in bubbly flow is much larger than that in single-phase flow and our model reproduces this result. Fig. 7 represents the turbulent viscosity given by the expression we proposed (Eq. (46)) and that computed from the model by Sato et al. (1981), (Eq. (47)). It appears that the turbulent viscosity issued from our second-order turbulence modelling is, in this case, much greater than that given by the Sato model. This viscosity, slightly greater than that for

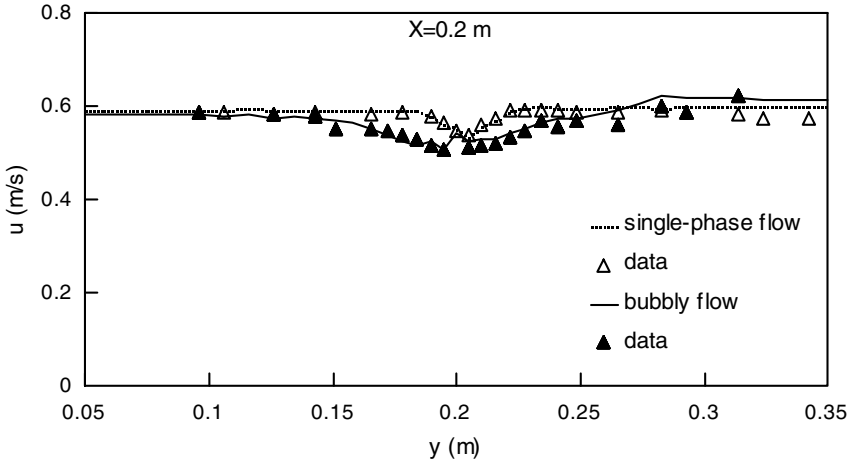

Fig. 5. Average longitudinal velocities in single-phase and bubbly wake flows at $X = 0.2$ m. Comparison of the numerical results with the experimental data of Roig (1993).

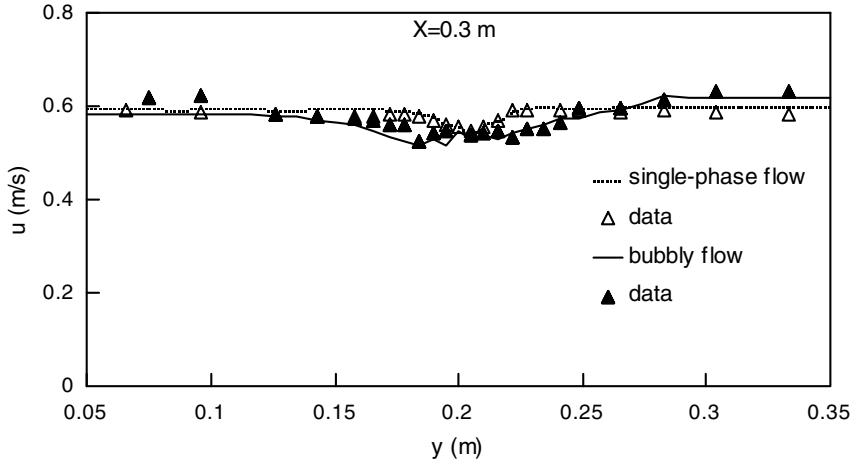

Fig. 6. Average longitudinal velocities in single-phase and bubbly wake flows at $X = 0.3$ m. Comparison of the numerical results with the experimental data of Roig (1993).

single-phase flow, is not sufficient to explain the great enhancement of the momentum spread observed in the experiment.

Figs. 8 and 9 show good agreement between the computed RMS longitudinal velocity profiles and the experimental data at $X = 0.2$ and 0.3 m from the inlet section. These numerical results show an adequate behaviour of the turbulence model in non-homogenous bubbly flow with an important amount of pseudo-turbulence. Since the relative velocity of the bubbles is initialised to their terminal velocity at the inlet section, the relative velocity is roughly constant throughout the flow field and the pseudo-turbulence given at the inlet is essentially transported by convection and turbulent diffusion.

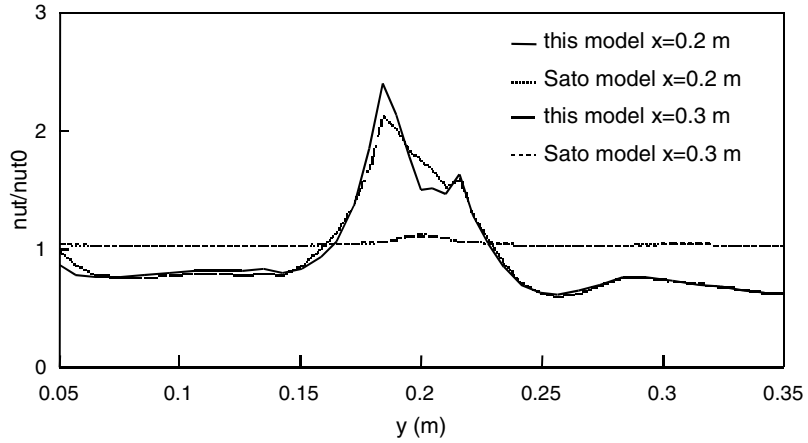

Fig. 7. Ratio of the "two-phase" flow turbulent viscosity to the "single-phase" one in bubbly wake at $X = 0.2$ and 0.3 m. Comparison of the present model with the model by Sato et al. (1981).

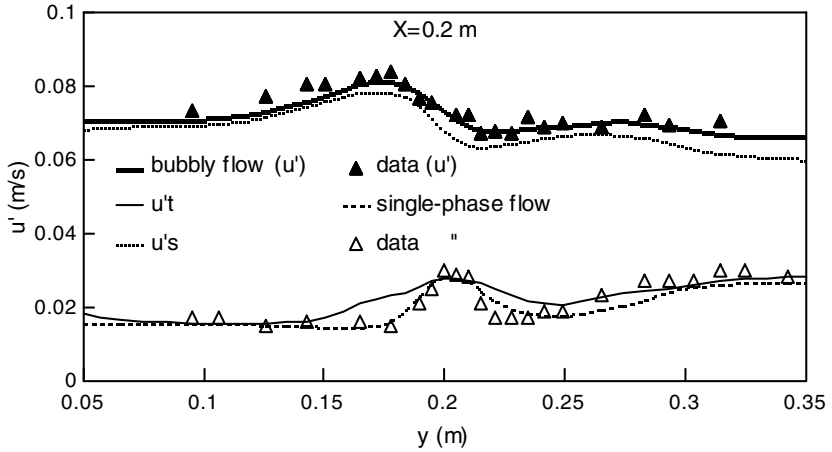

Fig. 8. RMS of longitudinal velocity in single-phase and bubbly wake flows at $X = 0.2$ m. Comparison of the numerical results with the experimental data of Roig (1993).

It should be noticed that test simulations indicate that the quality of the prediction of the average and of the fluctuating flow fields in bubbly flow is strongly linked to the quality of the prediction of the void fraction distribution. In this section the numerical results for the liquid phase were obtained for the case with the better prediction of void fraction (Run 111 as defined later). We discuss below the sensibility of the void fraction distribution to the interfacial force modelling.

5.2.2. Void fraction prediction

The experimental void fraction distribution shows a peak at the inlet section due to the development of the bubbly boundary layers on each side of the splitter plate. This peak decreases as

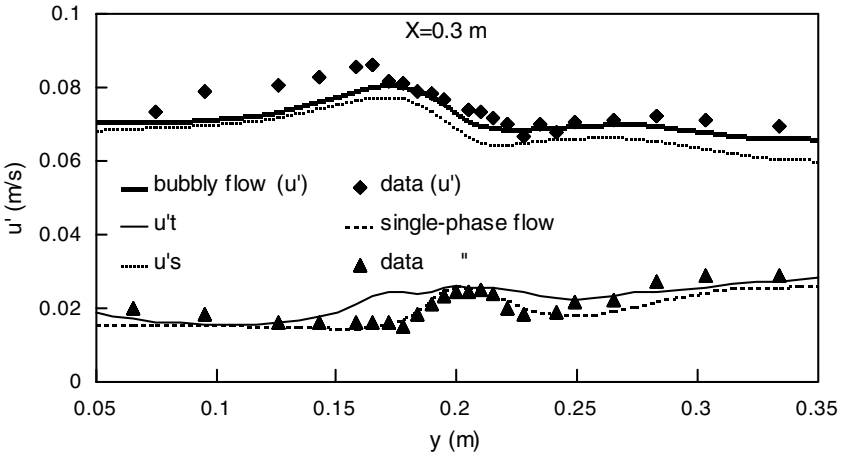

Fig. 9. RMS of the longitudinal velocity in single-phase and bubbly wake flows at $X = 0.2$ m. Comparison of the numerical results with the experimental data of Roig (1993).

the wake develops downstream. In order to analyse the role of the turbulence and of the interfacial forces in the phase distribution phenomena, different simulations were carried out with various interfacial momentum transfer models.

We first describe tests with the interfacial model that only considers the turbulent contribution of the interfacial momentum transfer through a diffusion term proportional to the gradient of the void fraction. We then examine the effect of the turbulent correlation resulting from the added mass force in the interfacial momentum transfer balance.

In the first two simulation sets the non-linear terms arising from the added mass effects are ignored. In the first set of simulations (RUN000, RUN001, RUN002 and RUN003) we left out the lift force and we tested the effect of the void fraction dispersion term appearing in the drift velocity. This one was modelled using Eq. (35) and the coefficient C_{DT} was first fixed to zero in RUN000 and then increased progressively in RUN001, RUN002 and RUN003. In the second set of simulations (RUN010, RUN011, RUN012 and RUN013) we kept the same conditions as before and we introduced the mean lift force with a coefficient $C_L = 0.25$, according to the experiment by Lance and Naciri (1992). The different simulations are summarised in Table 2. In the Figs. 10–13, the numerical results are compared with the experimental profiles of the void fraction at $X = 0.06$ and 0.2 m from the edge of the splitter plate.

In simulation RUN000, only the mean contributions of the added mass and of the drag forces were taken into account and the only turbulence effect came from the pressure term. While this interfacial momentum model is able to predict the void fraction distribution near the inlet section (at $X = 0.06$ m), Fig. 10, because it conserves the memory of the inlet section, it cannot reproduce

Table 2
Simulations without interfacial non-linear terms

	$C_{DT} = 0$	$C_{DT} = 1$	$C_{DT} = 5$	$C_{DT} = 15$
$C_L = 0$	RUN000	RUN001	RUN002	RUN003
$C_L = 0.25$	RUN010	RUN011	RUN012	RUN013

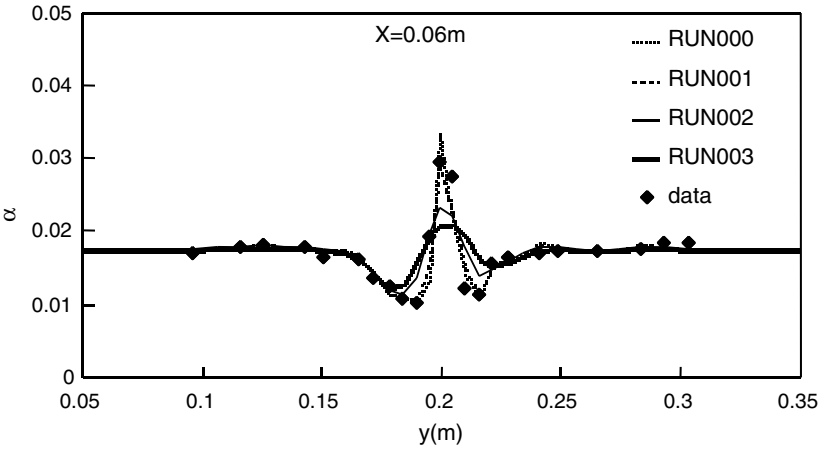

Fig. 10. Void fraction profiles in bubbly wake at $X = 0.06$ m; simulations without the non-linear added mass term and without the lift force. Comparison of the numerical results with the experimental data of Roig (1993).

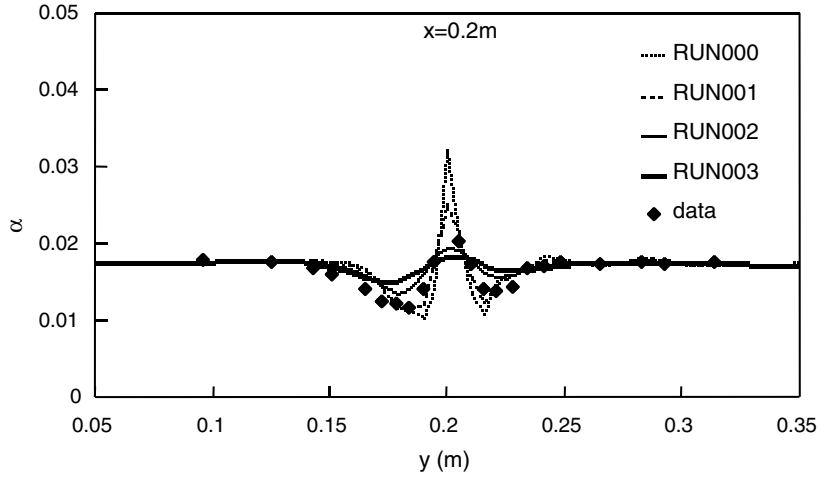

Fig. 11. Void fraction profiles in bubbly wake at $X = 0.2$ m; simulations without the non-linear added mass term and without the lift force. Comparison of the numerical results with the experimental data of Roig (1993).

the decrease of the void fraction peaking observed in the experiment between sections $X = 0.06$ and 0.2 m, Fig. 11. The dispersion term introduced in (RUN001, RUN002 and RUN003) yields a simple diffusion effect. When this dispersion model succeeds in reproducing the level of the void fraction peaking, it correlatively spreads the void fraction in each side of the void fraction peak and fails to maintain the troughs of void fraction at each side of the peak as observed in the experiment.

The lift force, introduced with a coefficient $C_L = 0.25$ in (RUN010, RUN011, RUN012 and RUN013), has no supplementary visible effect on the void fraction peaking because the position of the peak falls within the minimum of the velocity profile where the lift force is zero, (Figs. 12

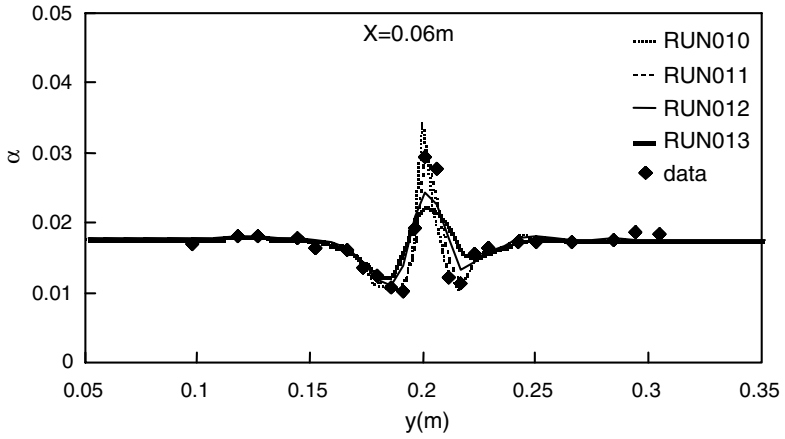

Fig. 12. Void fraction profiles in bubbly wake at $X = 0.06$ m; simulations without the non-linear added mass term and with the lift force. Comparison of the numerical results with the experimental data of Roig (1993).

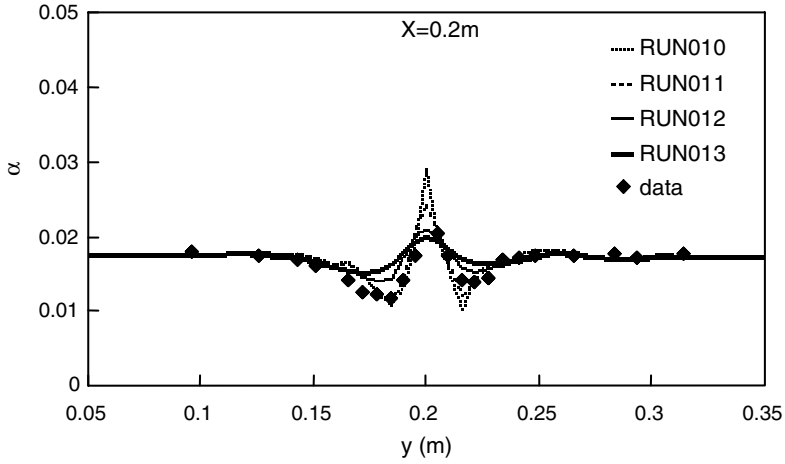

Fig. 13. Void fraction profiles in bubbly wake at $X = 0.2$ m; simulations without the non-linear added mass term and with the lift force. Comparison of the numerical results with the experimental data of Roig (1993).

and 13). Since the bubbles have no inertia (because of the low density of the gas), the action of the lift force is limited to the velocity gradient zones.

In a last set of simulations (RUN100, RUN101, RUN110 and RUN111), we introduced the turbulent correlations resulting from the added mass force. In simulation RUN100 the lift force and the dispersion effect are ignored. The dispersion term was introduced in simulation RUN101 with a coefficient $C_{DT} = 0.5$ and the lift force was introduced in simulation RUN110 with the coefficient $C_L = 0.25$. In simulation RUN111 the lift force and the dispersion effect are simultaneously taken into account. The different simulations are summarised in Table 3 and the Figs. 14–16 show the void fraction profiles obtained in these simulations at $X = 0.06$, 0.2, 0.3 m from the edge of the splitter plate.

Table 3
Simulations with interfacial non-linear terms

	RUN100	RUN101	RUN110	RUN111
C_{DT}	0	0.5	0	0.5
C_L	0	0	0.25	0.25

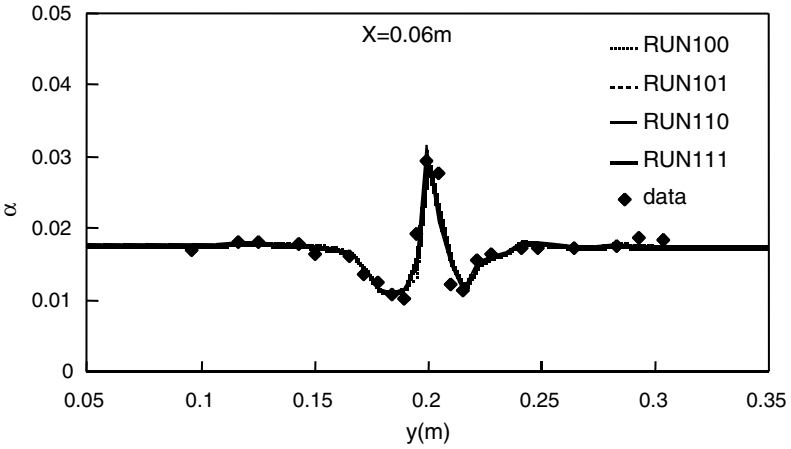

Fig. 14. Void fraction profiles in bubbly wake at $X = 0.06$ m; simulations with the non-linear added mass term. Comparison of the numerical results with the experimental data of Roig (1993).

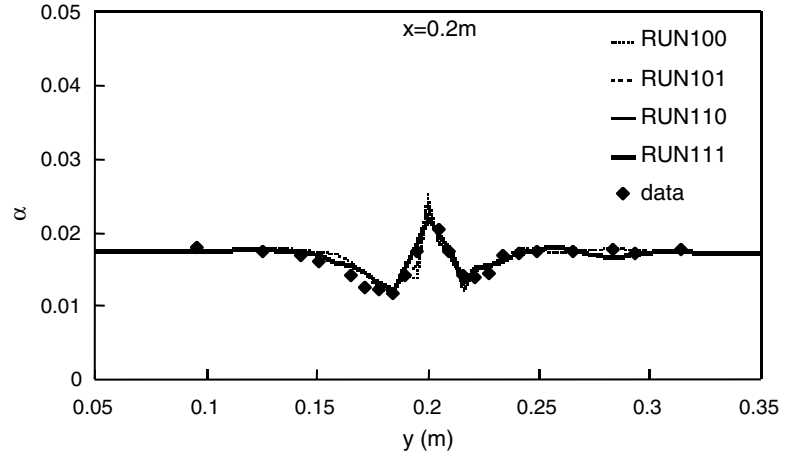

Fig. 15. Void fraction profiles in bubbly wake at $X = 0.2$ m; simulations with the non-linear added mass term. Comparison of the numerical results with the experimental data of Roig (1993).

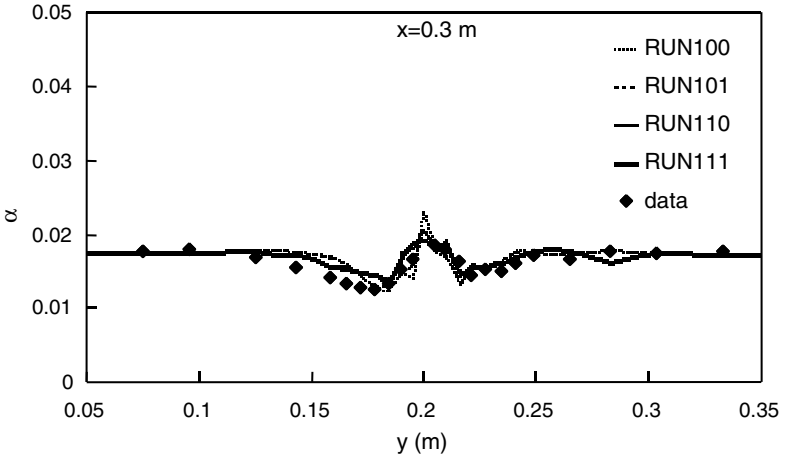

Fig. 16. Void fraction profiles in bubbly wake at $X = 0.3$ m; simulations with the non-linear added mass term. Comparison of the numerical results with the experimental data of Roig (1993).

This last set of simulations clearly shows the role-played by the non-linear added mass terms in the phase distribution phenomena. Indeed, we note that the decrease of the void fraction peaking is well reproduced and the void fraction troughs on each side of the void fraction peak are well predicted by the model: these troughs coincide precisely with the change of the turbulence profile slopes where the action of the non-linear terms is inverted (see Figs. 8 and 9). The dispersion term with a coefficient $C_{DT} = 0.5$ has a small effect; it should be reminded that with larger coefficients, the diffusion effect due to the dispersion term fills the troughs of void fraction on each side of the peak. Finally we noted once again that the lift force has no strong effect on void fraction peaking.

6. Conclusions

We have described an Eulerian–Eulerian two-fluid model developed for gas–liquid bubbly flows. This model, based on the closure of the average equations by a transport equation for the Reynolds stress tensor, improves the representation of the interaction between phases by introducing turbulent contributions in the expression of the force exerted by the liquid on the bubbles. The modelling of turbulence is based on the decomposition of the Reynolds stress tensor in the liquid phase into two parts: a turbulent dissipative part and a pseudo-turbulent non-dissipative part and we have written a transport equation for each part. This decomposition makes it possible to model the specific scales involved in each part and allows us to correctly describe the effects of the bubbles on the structure of liquid turbulence. The numerical results show an adequate behaviour of the model in homogenous and non-homogenous turbulence: the agitation of the bubbles induces on one hand an enhancement of the turbulent intensity and on the other hand a modification of the characteristic scale of eddy stretching that leads to an attenuation of the shear stress. The reduction of the second-order closure modelling of turbulence yields a new formulation for the turbulent viscosity that allows us to represent these effects.

The different simulations of the bubbly wake with various interfacial transfer models allows us to analyse the part played by the interfacial forces in the bubbles migration phenomenon: it appears that the turbulent correlations resulting from the added mass force are particularly significant with respect to the phase distribution phenomena.

Obviously, the two-fluid model, developed for dispersed bubbly flows, improves the representation of the interaction between phases and leads to a better prediction of bubbly flows. Nevertheless, some limitations inherent in the model formulation subsist. The main limitation is related to the formulation of the interfacial terms in the momentum equations. The interfacial term formulation assumes that the bubble diameter is relatively small compared to the smallest turbulent scales in the liquid and the expression of the instantaneous force exerted by the continuous phase on the bubbles is only valid for bubbles with low deformation and weak hydrodynamic interactions (low void fraction). Another important limitation of the model, related to the bubble size and hydrodynamic interactions, concerns the turbulence modelling: It is a matter of the linear decomposition of the Reynolds stress tensor and of the hypothesis of turbulence production and dissipation equilibrium in the bubble wake. In our opinion it is difficult at the present time to examine other closure hypotheses without new experiments and without decisive contributions from advanced numerical simulation methods (e.g. direct numerical simulation and large eddy simulation).

References

Auton, T.R., Hunt, J.C.R., Prud'Homme, M., 1988. The force exerted on a body in inviscid unsteady non-uniform rotational flow. J. Fluid Mech. 197, 241–257.

Bel Fdhila, R., Simonin, O., 1992. Eulerian prediction of a turbulent bubbly flow downstream of a sudden pipe expansion. Workshop on Two-phase flow predictions, 30 March–2 April, Erlangen.

Biesheuvel, A., Van Wijngaarden, L., 1984. Two-phase flow equation for a dilute dispersion of gas bubbles in liquid. J. Fluid Mech. 148, 301–318.

Chahed, J., Masbernat, L., 1998a. Effets des parois sur la distribution de taux de vide dans les écoulements à bulles. C.R. Acad. Sci. 326 (Série II b), 719–726.

Chahed, J., Masbernat, L., 1998b. Forces interfaciales et turbulence dans les écoulements à bulles. C.R. Acad. Sci.t 326 (Série II b), 635–642.

Chahed, J., Masbernat, L., Bellakhel, G., 1999. k-ϵ model for bubbly flows. 2nd Symposium on Two-Phase Flow Modelling and experimentation, May 23–25, Pisa, Italy.

Chahed, J., Masbernat, L., 2001. Numerical simulations of vertical and horizontal wall bounded turbulent bubbly flows. Fourth Int. Conf. on Multiphase Flow, May 27–June 1, New Orleans, Louisiana.

Clift, R., Grace, J.R., Weber, M.E., 1978. Bubbles, Drops and Particles. Academic Press, New York.

Csanady, G.T., 1963. Turbulent diffusion of heavy particles in the atmosphere. J. Atm. Sc. 20, 201–208.

Drew, D.A., Lahey, R.T., 1982. Phase distribution mechanisms in turbulent low-quality two-phase flow in circular pipe. J. Fluid Mech. 117, 91–106.

Gatignol, R., 1983. The faxen formulae for a rigid particle in an unsteady non-uniform stokes flow. Jounal de Mécanique Théorique et Appliquée 9, 143–160.

Hinze, J.O., 1975. Turbulence, second ed. Mc Graw-Hill, New York.

Lance, M., 1986. Etude de la turbulence dans les écoulements diphasiques dispersés. Thèse de doctorat ès Sciences, Université Claude Bernard, Lyon, France.

Lance, M., Bataille, J., 1991. Turbulence in the liquid phase of a uniform bubbly air water flow. J. Fluid Mech. 222, 95–118.

Lance, M., Marié, J.L., Bataille, J., 1991. Homogeneous turbulence in bubbly flows. J. Fluids Eng. 113, 295–300.

Lance, M., Naciri, A., 1992. Added mass and lift for a single bubble. First European Mechanics Conference, Cambridge, UK.

Lance, M., Lopez de Bertodano, M., 1992. Phase distribution phenomena and wall effects in bubbly two-phase flows. Third Int. Workshop on Two-Phase Flow Fundamentals, Imperial College, London, June 15–19.

Launder, B.E., Reece, G.J., Rodi, W., 1975. Progress in the development of a Reynolds stress turbulence closure. J. Fluid Mech. 68 (part 3), 537–566.

Lee, S.J, Lahey Jr., R.T., Jones Jr., O.C., 1989. The prediction of two phase turbulence and phase distribution phenomena using k, ϵ model. Jap. J. Multiphase Flow 3, 335–368.

Liu, T.J., Bankoff, S.G., 1990. Structure of air-water bubbly flow in a vertical pipe: I—Liquid mean velocity and turbulence measurements. Int. J. Heat Mass Transfer 36 (4), 1049–1060.

Lopez de Bertodano, M., Lee, S.J., Lahey, R.T., Drew, D.A., 1990. The prediction of two-phase turbulence and phase distribution using a Reynolds stress model. J. Fluids Eng. 112, 107–113.

Lopez de Bertodano, M., Lee, S.J., Lahey, R.T., Jones, O.C., 1994. Development of a k-ϵ model for bubbly two-phase flow. J. Fluids Eng. 116, 128–134.

Magnaudet, J., Rivero, M., Fabre, J., 1995. Accelerated flows past a rigid sphere or a spherical bubble. Part 1. Steady staining flow. J. Fluid. Mech. 284, 97–135.

Maxey, R., Riley, J., 1983. Equation of motion for a small rigid sphere in non-uniform flow. Phys. Fluids 26 (4), 883–889.

Morel, C., 1997. Modélisation multidimensionnelle des écoulements diphasiques gaz-liquide. Application à la simulation des écoulements à bulles ascendants en conduite verticale. Thèse de doctorat de l'Ecole Centrale de Paris.

Moursali, E., Marié, J.L., Bataille, J., 1995. An upward turbulent bubbly layer along a vertical flat plate. Int. J. Multiphase Flow 21, 107–117.

Rivero, M., Magnaudet, J., Fabre, J., 1991. Quelques résultats nouveaux concernant les forces exercées sur une inclusion sphérique par un écoulement accéléré. C. R. Acad. Sci. t312 (série II), 1499–1506.

Roig, V., 1993. Zones de mélange d'écoulements diphasiques à bulles. Thèse de docteur de l'Institut National Polytechnique de Toulouse.

Roig, V., Suzanne, C., Masbernat, L., 1998. Experimental investigation of a turbulent bubbly mixing layer. Int. J. Multiphase Flow 24, 35–54.

Sato, Y., Sadatomi, L., Sekoguchi, K., 1981. Momentum and heat transfer in two-phase bubbly flow. Int. J. Multiphase Flow. 7, 167–190.

Serizawa, A., Kataoka, I., Michiyoshi, I., 1992. Phase distribution in bubbly flow. In: Hewitt, G.F., Delhaye, J.M., Zuber, N. (Eds.), Multiphase Science And Technology, vol. 6. Hemisphere Publishing Corporation, New York, pp. 257–301.

Simonin, O., Viollet, P.L., 1989. Numerical study on phase dispersion mechanism in turbulent bubbly flows. Int. Conf. on Mechanics of Two-Phase Flows, June 12–15, Taipei, Taiwan.

Tennekes, H., Lumley, J.L., 1972. A first course in turbulence. MIT press, Cambridge, MA.

Wang, S.K, Lahey Jr., R.T., Jones Jr., O.C., 1987. Three dimensional turbulence structure and phase distribution measurements in bubbly two phase flows. Int. J. Multiphase Flow 13, 327–343.